Transport properties in Manganite

Phan Van-Nham and Tran Minh-Tien
Institute of Physics, National Center for Natural Science and Technology,
P.O. Box 429, Boho, 10000 Hanoi, Vietnam.

Transport properties in doped Manganite are studied by considering the simplified Double-exchange mechanism in the presence of diagonal disorder. It is modeled by a combination the Ising Double-exchange with Falicov-Kimball model. In this model, charge order ferromagnetic and transport quantities are presented by using Dynamical-mean field theory in the case of finite coupling Hund and disorder strenght. Those results suggest that, within this model the insulator phase can be stated in the range of below charge order temperature which is suitable with observation of experiment in manganites.

PACS numbers: 71.27.+a

I. INTRODUCTION

An enormous interest in the family of the doped manganice oxides $T_{1-x}D_xMnO_3$ (in which T is trivalent rare earth and D is divalent alkaline) in perovskite structure have been recent renewed.[1,2,3,4]As doping x and temperature T varied, the manganites show a very rich phase diagram involving phases with spin, charge and orbital order.[1,2,3,4]In the cubic lattice, the five-fold degenerate $3d$-orbitals of an isolated atom or ion are spilitted into a manifold of three lower energy (d_{xy}, d_{yz}, and d_{xz}), usually referred to as t_{2g} one mixing with the surrounding oxygens is included, and two higher energy states ($d_{x^2-y^2}$ and $d_{3z^2-r^2}$) called e_g state. Electron t_{2g} are usually located but electron e_g are itinerant so they create band energy. The correlation between t_{2g} and e_g electron is expressed by Double Exchange (DE) mechanism[5] inwhich two motions involving electrons moving from the oxygen atom to the Mn^{4+} ions and other one from the Mn^{3+} to the oxygen atom. The main feature of DE is cooperative effect where the motion of an itinerant electron favors the ferromagnetic (FM) ordering of local spin and, vice versa, the presence of the FM order facilitates the motions of the itinerant electron. The DE model has been studied in "one orbital" model because it is not only simplify but also contains enough degree of freedom to manifest the phenomena of DE mechanism which was envisioned in the early days of manganites studies.
Recent experiment observed in the Manganites have shown that the DE model alone can not explain the quantitative features of the temperature dependence of the resistivity through the entire temperature range[6]. To improve the theoretical understanding in Manganites, there are two proposed resolutions of this problem. The first one is a large Jahn-Teller lattice distortion which causes a metal-insulator transition (MIT) via strong polaronic narrowing of the conduction electron band. However, the Jahn-Teller lattice distortion makes the charge-ordering phase occurs before the FM transition temperature[7]which is not suitable with experimental observation at half-filling.[2,8]In the second proposed resolution, the insulating behavior is caused by a combination of both magnetic disorder and non-magnetic ionic disorder. The magnetic disorder arises from the random DE factor $\cos(\theta/2)$ in the electronic hoping (θ is the angle between local spins) which call off-diagonal. The non-magnetic comes from the ionic doping of the D^{2+} ion (i.e. from randomness at the chemical substituting T^{3+} by D^{2+}) which leads to a random local potential for the charge carriers. This disorder always presents in doped Manganite which called diagonal-disorder that can lead to Anderson localization of the charge carriers.[9]It is well known that, the diagonal-disorder can be modeled by the Falicov-Kimball (FK) model.[10] Although the FK model is simple, it contains a rich variety of phases which are controlled by electron interaction.[11,12]Incorporating the diagonal-disorder of FK type into DE model, one may expect that a disorder-order phase transition could present. When phase transition occurs, a CO-FM phase may be stabilized at low temperature[13] and the behaviors of transport coefficients can be more close with the experiment results. In this paper, the transport coefficients such as d.c. conductivity, thermal conductivity and thermal power of system are being studied by the Dynamical mean-field theory (DMFT)[14]. The DMFT have been extensively used for investigating strongly correlated electron system.[14]It is based on the fact that, the self-energy depends only on frequency in the infinite dimension limit. Using DMFT we found that the system stabilizes inhomogeneous ferromagnetic state at low temperature and gives us a fulfill picture of behaviors of the transport coefficients.
This paper is organized as follows:

II. MODEL AND TRANSPORT COEFFICIENTS

The system which we consider is described by the following Hamiltonian

$$H = -t \sum_{<ij>,\sigma} c^{\dagger}_{i\sigma} c_{j\sigma} - \mu \sum_{i\sigma} c^{\dagger}_{i\sigma} c_{i\sigma} - 2J_H \sum_i S^z_i s^z_i$$

$$+U\sum_{i\sigma} n_{i\sigma}n_{fi} + E_f\sum_i n_{fi}, \quad (1)$$

where $c^\dagger_{i\sigma}(c_{i\sigma})$ is the creation (annihilation) operator for an itinerant electron with spin σ at lattice site i. The first term in the Hamiltonian (1) represents the hoping between the nearest neighbors sites. t is the hoping integral and is scaled with the spatial dimension d in the limit $d\to\infty$ as[14]. $t=\frac{t^\star}{2\sqrt{d}}$. In the following we will take $t^\star=1$ as the unit of energy.[14] S^z_i is the z component of the local spin at lattice site i, it takes values $-\frac{3}{2},-\frac{3}{2}+1,...,\frac{3}{2}$, $s^z_i=\frac{1}{2}\sum_\sigma c^\dagger_{i\sigma}\sigma^z c_{i\sigma}$ with σ^z is the z- component of Pauli matrix is the spin of itinerant electron. n_{fi} is a classical variable that assumes the value 1(0) if site i is occupied by (is not occupied by) D^{2+} ion. U is the disorder strength and is mapped onto the difference in the local potential which spilits energetical favor of Mn^{3+} and Mn^{4+} ion, the expectation value $x=\sum_i\langle n_{fi}\rangle/N$ (N is the number od lattice sites) corresponds to the concentration of unfavorable Mn^{4+} sites. The chemical potential μ controls the carrier dopings, while E_{n_f} controls the fraction of the sites having the additional local potential. The condition $n+x=1$ where $n=\sum_{i\sigma}\langle n_{i\sigma}\rangle/N$ is electron doping is used which determines E_f for each doping n. The first three terms in the Hamiltonian (1) describe a simplified DE model which contains only the Ising-type interaction between the itinerant and local electrons. Within the DMFT the Ising type of the Hund interaction gives basically same results as the ones of the Hund interaction of clasical spins.[14]The simplication does not allow any spin-flip processes, which can be important at low temperature where spin-wave excitations may govern the thermodynamics of the system. However, within the DE model the DMFT calculations for quantum spins does not show significant differences from the one for clasical spins.[15,16]The last two terms in the Hamiltonian (1) describe a binary randomness of the T-site substitution. They together with the hoping term of itinerant electrons form the FK model.[17,18]

Transport coefficients are calculated within a Kubo-Greenwood formalism[19], in which the dc-conductivity σ, thermal power S and the thermal conductivity κ can be expressed with the relevant correlation functions of the current operators. We have[19]

$$\sigma=\frac{e^2}{T}L^{11}, \quad (2)$$

$$S=-\frac{1}{eT}\frac{L^{12}}{L^{11}}, \quad (3)$$

$$\kappa=L^{22}-\frac{(L^{12})^2}{L^{11}}. \quad (4)$$

where coefficients L^{11},L^{12} and L^{22} are determined from the analytic continuation of the relevant current-current correlation function at zero frequency, i.e.,

$$L^{ij}=\lim_{\nu\to 0}T\mathrm{Im}\frac{\overline{L}^{ij}(\nu)}{\nu}. \quad (5)$$

Here $\overline{L}^{ij}(\nu)$ is the relevant current-current correlation functions

$$\overline{L}^{11}(i\nu_n)=\int_0^\beta d\tau e^{i\nu_n\tau}\langle T_\tau\mathbf{j}(\tau)\mathbf{j}(0)\rangle, \quad (6)$$

$$\overline{L}^{12}(i\nu_n)=\int_0^\beta d\tau e^{i\nu_n\tau}\langle T_\tau\mathbf{j}(\tau)\mathbf{j}_Q(0)\rangle, \quad (7)$$

$$\overline{L}^{22}(i\nu_n)=\int_0^\beta d\tau e^{i\nu_n\tau}\langle T_\tau\mathbf{j}_Q(\tau)\mathbf{j}_Q(0)\rangle. \quad (8)$$

Where $\mathbf{j}$ and $\mathbf{j_Q}$ are the particle-current operator and the heat-current operator, respectively. The particle-current operator is defined by taking commutator of the Hamiltonian with the polarization operator $\sum_i\mathbf{R}_i n_i$.[19]In our model, there are two inequivalent sublattice A and B so it is useful to divide Hamiltonian (1) into four terms.

$$H=H_A+H_B+H_{AB}+H_{BA}, \quad (9)$$

with $H_\alpha=U\sum_\sigma n_{f\alpha}n_{\alpha\sigma}-2J\sum_\sigma S^z_\alpha s^z_\alpha+E_f\sum n_{f\alpha}$ where $\alpha=A(B)$ for sublattice A(B) expresses the interactions of sublattice A(B) and $H_{AB}=-t\sum_\sigma a^\dagger_\sigma b_\sigma$, $H_{BA}=-t\sum_\sigma b^\dagger_\sigma a_\sigma$ with $a^\dagger_\sigma,a_\sigma$ $(b^\dagger_\sigma,b_\sigma)$ are creation and annihilation operator for sublattice A(B) respond to the hopping between A and B site. After some algebraic calculations we obtain.

$$\mathbf{j}=\sum_{\mathbf{q}} v_{\mathbf{q}}(a^\dagger_{\mathbf{q}\sigma}b_{\mathbf{q}\sigma}+b^\dagger_{\mathbf{q}\sigma}a_{\mathbf{q}\sigma}) \quad (10)$$

in momentum representation, where velocity $v_{\mathbf{q}}=\bigtriangledown_{\mathbf{q}}\epsilon(\mathbf{q})$ and $\epsilon(\mathbf{q})$ is the dispersion of the non-interacting electrons. The heat-current $\mathbf{j}_Q$ can be determined by the energy current $\mathbf{j}_E$ and the particle current $\mathbf{j}$, $\mathbf{j}_Q=\mathbf{j}_E-\mu\mathbf{j}$. The energy-current is defined by taking commutator of the Hamiltonian with the energy polarization operator $\sum_i\mathbf{R}_i h_i$ (where $H=\sum_i h_i$). We obtain

$$\mathbf{j}_Q=\sum_{\mathbf{q}\sigma}\mathbf{v}_{\mathbf{q}}[\epsilon(\mathbf{q}-\mu](a^\dagger_{\mathbf{q}\sigma}b_{\mathbf{q}\sigma}+b^\dagger_{\mathbf{q}\sigma}a_{\mathbf{q}\sigma})$$
$$-\frac{1}{2}\sum_{\mathbf{q},\mathbf{q}'\sigma}W(\mathbf{q}-\mathbf{q}')(\mathbf{v}_{\mathbf{q}'}+\mathbf{v}_{\mathbf{q}})(a^\dagger_{\mathbf{q}\sigma}b_{\mathbf{q}'\sigma}+b^\dagger_{\mathbf{q}\sigma}a_{\mathbf{q}'\sigma}), \quad (11)$$

where $W(\mathbf{q}-\mathbf{q}')=\frac{1}{N}\sum_i(J\sigma S^z_i-n_fU)e^{-i(\mathbf{q}-\mathbf{q}')\mathbf{R}_i}$.

Using the equation of motion (EOM) technique[17] we can write the heat-current operator in the form

$$\mathbf{j}_Q = \lim_{\tau'\to\tau^-} \frac{1}{2}\sum_{\mathbf{q},\sigma}(\frac{\partial}{\partial\tau} - \frac{\partial}{\partial\tau'})v_{\mathbf{q}} \times(a^\dagger_{\mathbf{q}\sigma}(\tau)b_{\mathbf{q}\sigma}(\tau') + b^\dagger_{\mathbf{q}\sigma}(\tau)a_{\mathbf{q}\sigma}(\tau')). \quad (12)$$

Substubting $\mathbf{j}$ and $\mathbf{j}_Q$ from (10) and (11) into (6)(7) and (8), the transport coefficients are able to be calculated in the canceling of the vertex correction at infinite dimension limit[16,20]

$$L^{11} = T\sum_\sigma \int d\epsilon\rho(\epsilon)\int d\omega\left(-\frac{\partial f(\omega)}{\partial\omega}\right)A_{A\sigma}(\epsilon,\omega)A_{B\sigma}(\epsilon,\omega), \quad (13)$$

$$L^{12} = T\sum_\sigma \int d\epsilon\rho(\epsilon)\int d\omega\left(-\frac{\partial f(\omega)}{\partial\omega}\right)A_{A\sigma}(\epsilon,\omega)A_{B\sigma}(\epsilon,\omega)\omega, \quad (14)$$

$$L^{22} = T\sum_\sigma \int d\epsilon\rho(\epsilon)\int d\omega\left(-\frac{\partial f(\omega)}{\partial\omega}\right)A_{A\sigma}(\epsilon,\omega)A_{B\sigma}(\epsilon,\omega)\omega^2. \quad (15)$$

where $f(\omega) = 1/(\exp(\omega/T)+1)$ is Fermi-Dirac distribution function and $A_{\alpha\sigma}(\epsilon,\omega) = -\frac{1}{\pi}\mathrm{Im}G_{\alpha\sigma}(\epsilon,\omega)$ is the spectral function of the Green function for the intinerant electron for sublattice A or B. In that way, the transport coefficients are fully determined by the single particle spectral function.

III. DMFT IN SDE WITHIN FK MODEL

We solve model (1) by the DMFT. The DMFT is based on the infinite dimension limit. In the infinite dimension limit the self energy is pure local and does not depend on momentum. By using the standard technique[14] the matrix Green function of the itinerant electrons satisfies in the following form

$$\widehat{G}^{-1}_\sigma(\mathbf{k},i\omega) = \begin{pmatrix} \omega_{\mathbf{k}} + \mu - \Sigma^A_\sigma(\omega) & -\epsilon(\mathbf{k}) \\ -\epsilon(\mathbf{k}) & \omega_{\mathbf{k}} + \mu - \Sigma^B_\sigma(\omega)\end{pmatrix}, \quad (16)$$

where $\varepsilon(\mathbf{k})$ is the dispersion of free itinerant electrons on a hypercubic lattice, $\Sigma^{A(B)}_\sigma(\omega)$ is the self energy for sublattice A(B). The self energy is determined by solving an effective single-site problem. The effective action for this problem is

$$S_{\alpha\mathrm{eff}} = -\int d\tau\int d\tau'\sum_\sigma c^\dagger_{\alpha\sigma}(\tau)\mathcal{G}^{-1}_{\alpha\sigma}(\tau-\tau')c_{\alpha\sigma}(\tau') - \int d\tau\sum_{\sigma n_{f\alpha}}[JS^z\sigma + \mu - Un_{f\alpha}]c^\dagger_{\alpha\sigma}(\tau)c_{\alpha\sigma}(\tau) + E_f n_{f\alpha}, \quad (17)$$

where $c_{\alpha\sigma} = a_\sigma(b_\sigma)$ if $\alpha = A(B)$ and similar to $c^\dagger_{\alpha\sigma}$, $\mathcal{G}_{\alpha\sigma}(\tau-\tau')$ is the Green function of a effective medium for each sublattice A or B. It plays as the base Green function of the effective problem. The local Green function also satisfies the Dyson equation.

$$G^{-1}_{\alpha\sigma}(\omega) = \mathcal{G}^{-1}_{\alpha\sigma}(\omega) - \Sigma_{\alpha\sigma}(\omega). \quad (18)$$

The local Green function $G_{\alpha\sigma}(\omega)$ of the effective single-site problem is solely determined by the partition function. It can be calculated by.

$$G_{\alpha\sigma}(i\omega_n) = \frac{\delta\mathcal{Z}_{\alpha\mathrm{eff}}}{\delta\mathcal{G}^{-1}_{\alpha\sigma}(i\omega_n)}, \quad (19)$$

where Z_{eff} is the partition function and $\omega_n = (2n+1)\pi T$ is the Matsubara frequency. Within the effective single-site problem, the partition function becomes

$$\mathcal{Z}_{\alpha\mathrm{eff}} = \mathrm{Tr}\int Dc^\dagger_{\alpha\sigma}Dc_{\alpha\sigma}e^{-S_{\alpha\mathrm{eff}}}, \quad (20)$$

where the trace is taken over S_z and $n_{\alpha f}$. This partition function can be calculated exactly. Indeed, the Dynamics of the local spin S^z and impurity $n_{\alpha f}$ involved in the effective action (17) independently, we could take the trace over S^z and $n_{\alpha f}$ in partition function(20) independently. This is similar to DMFT solving the FK model[21], we obtain

$$\mathcal{Z}_{\alpha\mathrm{eff}} = 4\sum_{m,n_{\alpha f}}\exp\left\{\sum_{n,\sigma}(\ln[\mathcal{G}^{-1}_{\alpha\sigma}(i\omega_n) + J_H\sigma m + \mu - Un_{\alpha f}] - \ln i\omega_n)e^{i\omega_n\theta^+}\right\}e^{E_f n_{\alpha f}\beta}, \quad (21)$$

where $m = -\frac{3}{2}, -\frac{3}{2}+1, \ldots \frac{3}{2}$ are projections of the local spin S_z on z axit.
Using Eq.(19) we obtain the local Green function on real axis after taking analytical continuation

$$G_{\alpha\sigma}(\omega) = \sum_{m,n_{\alpha f}} \frac{w_{m\alpha}}{\mathcal{G}^{-1}_{\alpha\sigma}(\omega) + J_H\sigma m + \mu - Un_{\alpha f}}, \tag{22}$$

where

$$w_{m\alpha} = \frac{1}{\mathcal{Z}_{\text{eff}}} \exp\left\{-\beta \int d\omega f(\omega) \frac{1}{\pi} \text{Im} \sum_{\sigma} \ln[\mathcal{G}^{-1}_{\sigma}(\omega) + J_H\sigma m + \mu - Un_{\alpha f}]\right\}. \tag{23}$$

Equation (22) is similar to the one with the classical local spin.[15]It can be considered as a generalized formula of the local Green function for any value of the local spin. The self-consitent condition of the DMFT requires the local Green function of the original lattice. That mean,

$$G_{\alpha\sigma}(\omega) = \frac{1}{N}\sum_{\mathbf{k}} G_{\alpha\sigma}(\mathbf{k},\omega). \tag{24}$$

From equation (16) we obtain

$$G_{\alpha\sigma}(\omega) = \zeta_{\overline{\alpha}\sigma} \int d\epsilon \rho(\epsilon) \frac{2}{\zeta_{A\sigma}\zeta_{B\sigma} - \epsilon^2}, \tag{25}$$

where $\alpha = A, B$ and $\overline{\alpha} = B, A$, $\zeta_{\alpha\sigma} = \omega + \mu - \Sigma^{\alpha}_{\sigma}(\omega)$.
Eqs. (18)(22), and (25) form the complete set of equations, which self-consistently determines the self-energy and the Green function for each sublattice A and B.

IV. NUMERICAL RESULTS

In this section we present the solution of the self-consistent DMFT Eqs.(18)(22), and (25). The self-energy and the Green function are obtained by iterations.[21]With the obtained Green function, we calculate the d.c. resistivity, thermal conductivity, and thermal power by Eqs. (13)(14), and (15).
In Fig.1a we present the magnetization $m_{A(B)} = \sum_{i\in A(B)}(n_{i\uparrow} - n_{i\downarrow})/N$ of sublattice A(B) as the function of temperature and we also plot the dependence of charge-order parameter $\Delta = (n_A - n_B)$ (where $n_{A(B)} = \sum_{i\in A(B)\sigma} n_{i\sigma}/N$) on temperature in a case where the filling of the localized and intinerant electron is equal 0.5 with $J = 8$ and various of disorder strengths U. In this paper, we only concentrate in the case of normal manganites where the Hund coupling dominates with the disorder strenght that mean $J_H \ll U$. When U is large, it shows that, below critical temperature the magnetization of both-sublattices exists. They equal to each other until another critical temperature where the charge-order parameter exist. That mean, at low temperature, system is in the charge board CO-FM state. In this phase the charge-order coexists in the FM state which had been observed.[8]But with the small value of U, the CO-phase disappears, and only FM phase exists. With those coexistances of phases, the dependence of transport coefficients on temperature behaves as expected. In Fig.1b the behaviors of resistivity in temperature range is plotted.
It shows that, in high temperature range, the dependence of resistivity on temperature shows the metallic behavior ($d\rho/dT > 0$). Immediately below the transition temperature ferromagnetic T_C the resistivity declines with decreasing temperature due to the reduction of the magnetic contribution to electron scattering. Hence, at low temperature system is in FM phase. But when temperature decreases below CO transition temperature, the system changes the phase to insulator ($d\rho/dT < 0$) in the large U case. In the case of small U our system is in metallic through the entire temperature range which is the same results as in the SDE model[21].
The kinks at T_C and T_{CO} temperature in the resistivity curve indicate the FM and CO transitions. The last two Fig.1(c and d) show the dependence of the thermal conductivity and thermal power vs temperature. They behaviors express as expected. At low temperature the thermal conductivity decreases and disappears when $T = 0$. When temperature increases, the thermal conductivity has a peak at the temperature which decreases with the decreasing of U, but with the large of T the thermal conductivity slowly increases and is reputed without depending on disorder strength U. The thermal power also behaves as expected. At low temperature, it is negative that because of the priority of hole-carrier particles and shows a sharp peak. When T is increased, the thermal power changes the sign and increases. Those results had been obtained in the FK model.[18]

Above results can be understood clearly if we plot the DOS of itinerant electron. In Fig.2 the DOS for half filling $n_f = n_e = 0.5$ case with $J = 8, U = 0.5$ for various temperature is expressed. At low temperature ($T < T_{CO}$) the DOS of each sublattice and each spin direction are distincted, that mean our system is in CO-FM phase. At temperature $T_{CO} < T < T_C$ the distinction between sublattice A and B disappears but ones for spin direction are still on distinction which expresses the FM phase only. When the temperature

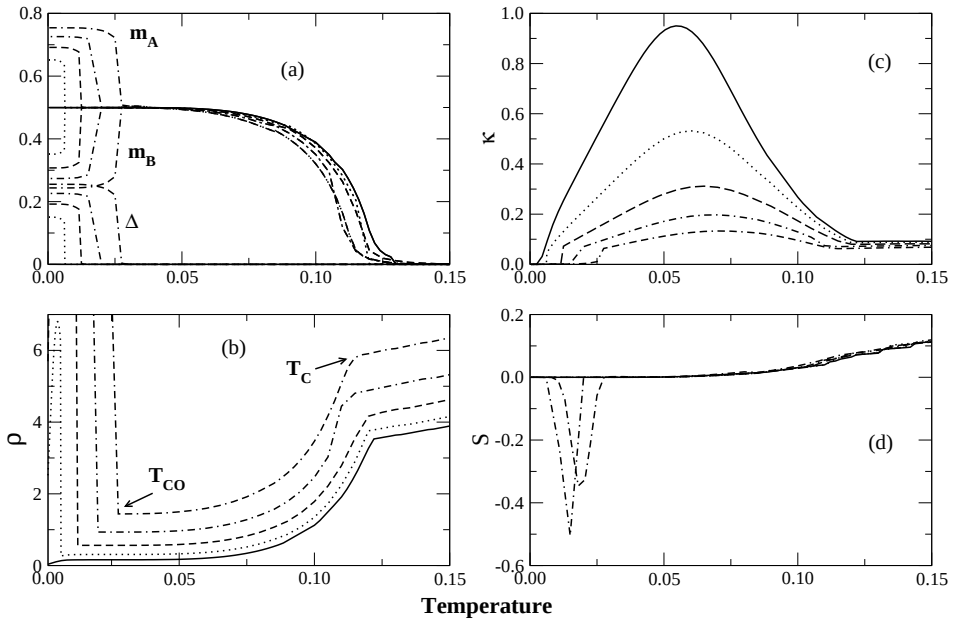

FIG. 1: Temperature dependence of the magnetization $m_A(m_B)$ for sublattice A(B) and charge-order parameter Δ(a), d.c. resistivity(b), thermal-conductivity(c), and thermal-power(d) in a case of half-filling ($n_e = n_f = 0.5$) and $J = 8.0$ for different disorder strength U: $U = 0.1$ (solid line), $U = 0.2$ (dotted), $U = 0.3$ (dashed line), $U = 0.4$ (chain-dotted), and $U = 0.5$ (double chain-dotted).

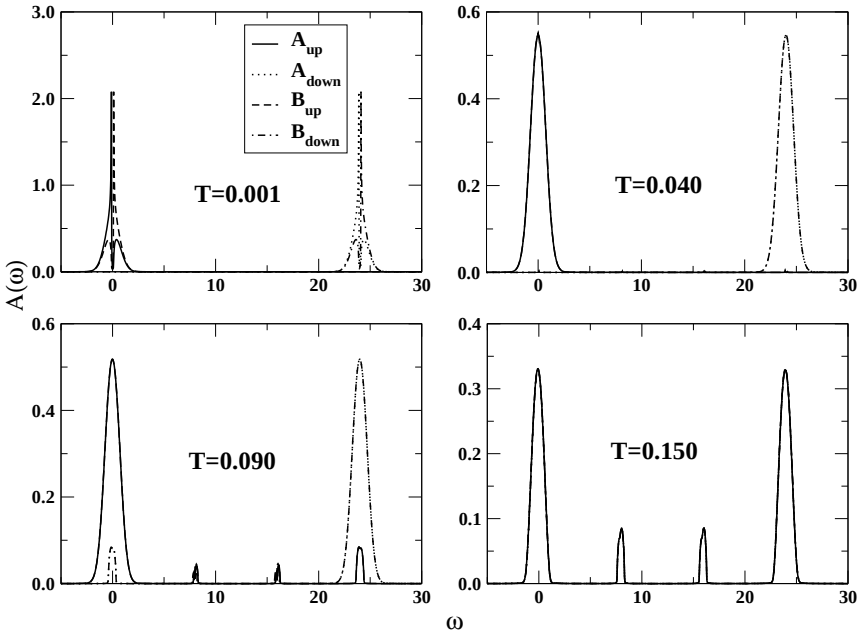

FIG. 2: Density of State of initerant electron in the case of of half-filling ($n_e = n_f = 0.5$), $J = 8.0$, and $U = 0.5$ for various temperatures

is larger ($T > T_C$), all DOS of each sublattice and each spin direction are concided which decribed the Paramagnetic phase. In all temperatures above T_{CO} the Fermi-level states in band energy so our system is in metallic phase but with temperature is smaller than T_{CO} the DOS are depleted at Fermi-level that mean there occurs the gap which expresses the insulator phase.

The DOS for various U of spin up only, at low temperature are also expressed in Fig.4. One can see that, for weak coupling the DOS is essentially unchanged from

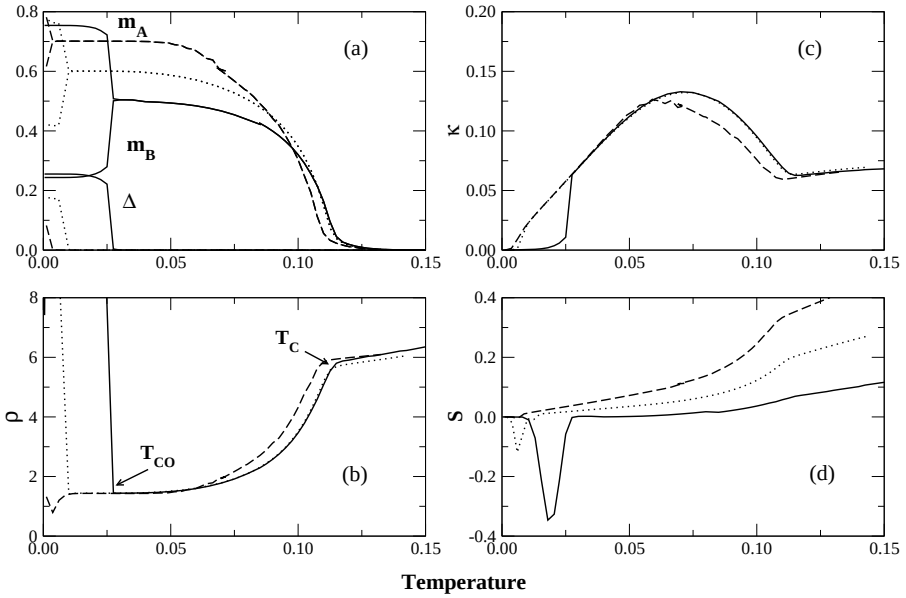

FIG. 3: Temperature dependence of the magnetization $m_A(m_B)$ for sublattice A(B) and charge-order parameter Δ(a), d.c. resistivity(b), thermal-conductivity(c), and thermal-power(d) in a case of half-filling ($n_e + n_f = 1.0$) $U = 0.5$, and $J = 8.0$ but for different concentrations: $n = 0.5$ (solid line), $n = 0.6$ (dotted), and $n = 0.7$ (dashed line).

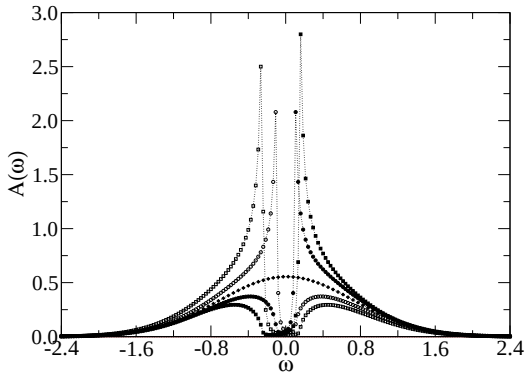

FIG. 4: Density of State of itinerant spin-up electron only in the case of of half-filling ($n_e = n_f = 0.5$), $J = 8.0$, and some values of disorder strength: $U = 0.1$ (diamond), $U = 0.4$ (square), and $U = 0.5$ (circle) (opened(filled) for sublattice A(B)) at low temperature $T = 0.001$.

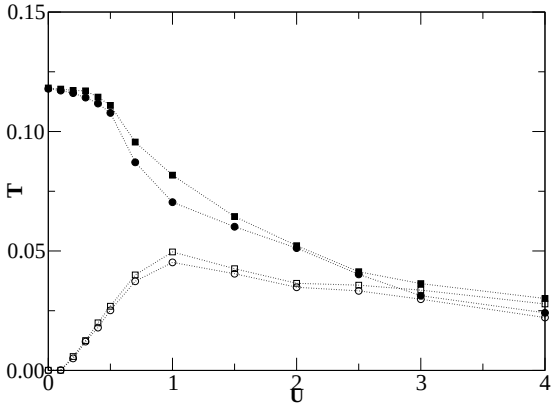

FIG. 5: The critical temperature T_C (filled) and T_{CO} (opened) as a function of disorder strength U for $J = 8.0$ (square) and $J = 6.0$ (circle).

the SDE model, but as U is increased further, the gap of DOS appears and its width increases. This result is precisely the kind of metal-insulator transition that Mott envisioned.

The similar results for various itinerant concentration n_e also are plotted in the Fig.3. It shows that, when n_e increases the T_{CO} and T_C decrease which also is obtained in the infinite of Hund coupling J[13]. In Fig.5 the dependence of the critical temperature of the FM and CO phase transition on disorder strength are presented. That means the disorder substantially decrease T_C of the FM transition. At the same time, with increasing U, critical temperature of the CO phase transition first increases, reaches its maximal value and decreases later. This behavior of critical temperature of the CO phase transition is similar to the one in FK model[12].

In the large strength of U the T_{CO} and T_C are close in on the same value but T_{CO} still is smaller than T_C. That means, the CO state is stabilized in the FM phase at low temperature. This results are observed in experiment[8].

V. CONCLUSION

In this paper, we have considered the transport properties in the SDE model with the combination of diagonal-disorder by employing the DMFT. It is found that the FM and CO states are stabilized at low temperature and expected behavior of the transport coefficients are expressed respectively. Those results improve the one for SDE model so they describe more suitable of the transport properties in the Manganites. Although, the manganites are too complicate a system to be completely described by this simple model, the obtained transport properties qualitatively reproduce the ones observed in the manganites.

Acknowledgement
The authors grateful to Prof. Dr. Holger Fehske for the valuable discussions. This work is supported by the National Program of Basic Research on National Science, Project 4.1.2.

[1] M. B. Salamon and M. Jaime, Rev. Mod. Phys. **73**, 583 (2001).
[2] E. Dagotto, T. Hotta, and A. Moreo, Phys. Rep. **344**, 1 (2001).
[3] Y. A Izyumov and Y. N. Skryabin, Physics- Uspekhi **44**, 109 (2001).
[4] J. M. D. Coery, M. Viret, and S.Von Molnar, Adv. Phys. **48**, 167 (1995).
[5] F. Zhong, J. Dong, and Z. D. Wang, Phys. Rev. B **58**, 15310 (1998).
[6] A. J. Millis, R. B. Littlewood, and B. I. Shraimon, Phys. Rev. Lett. **74**, 5144 (1995).
[7] S. Yunoki, T. Hotta, and E. Dagotto, Phys. Rev. Lett. **84** 3714 (2000).
[8] J. C. Loudon, N. D. Mathur, and P. A. Midgley, Nature **420**, 797 (2002).
[9] R. Allub and B. Alascio, Solid State Commun. **99**, 66 (1996); Phys. Rev. B **55**, 14 113 (1997).
[10] L. M. Falicov and J. C. Kimball, Phys. Rev. Lett. **22** 997 (1969).
[11] T. Kennedy and E. H. Lieb, Physica A **138**, 320 (1986); *ibid.* **140**, 240 (1986).
[12] U. Brandt and C. Mielsch, Z. Phys. B **63**, 45 (1986); *ibid.* **67**, 43 (1987), *ibid.* **82**, 37 (1991).
[13] Tran Minh-Tien, cond-mat/0302328.
[14] A. Georges, G. Kotliar, W. Krauth, and M. J. Rozenberg, Rev. mod. Phys. **68**, 13 (1996).
[15] N. Furukawa, J. Phys. Soc. Ipn. **63**, 3214 (1994); *ibid.* **64**, 2754 (1995); *ibid.* **65**, 1174 (1996).
[16] K. Nagai, T. Momoi, and K. Kubo, J. Phys. Soc. Jpn. **69**, 1837 (2000).
[17] J. K. Freericks and V. Zlatic, cond-mat/0108500.
[18] J. K. Freericks and V. Zlatic, cond-mat/0301188.
[19] G. D. Mahan, "Many Particle Physics", 2nd edition, Plemum Press (1990).
[20] T. Pruschke, D. L. Cox, and M. Jarrell, Phys. Rev. B **47** 8553 (1993).
[21] Phan Van-Nham and Tran Minh-Tien, Mod. Phys. Lett. B Vol. **17**, No. 1 (2003) 39-47.